Liquid Crystals

Publication details, including instructions for authors and subscription information:
http://www.informaworld.com/smpp/title~content=t713926090

Interface influenced phase transitions of alkylcyanobiphenyl liquid crystals A calorimetric study

Germano Iannacchione[a]; Alfredo Strigazzi[b]; Daniele Finotello[a]
[a] Department of Physics and Liquid Crystal Institute, Kent State University, Kent, Ohio [b] Dipartimento di Fisica, Politecnico di Torino, and INFM, Unità di Torino, Torino, Italy

To cite this Article Iannacchione, Germano , Strigazzi, Alfredo and Finotello, Daniele(1993) 'Interface influenced phase transitions of alkylcyanobiphenyl liquid crystals A calorimetric study', Liquid Crystals, 14: 4, 1153 — 1161
To link to this Article: DOI: 10.1080/02678299308027823
URL: http://dx.doi.org/10.1080/02678299308027823

LIQUID CRYSTALS, 1993, VOL. 14, NO. 4, 1153–1161

Interface influenced phase transitions of alkylcyanobiphenyl liquid crystals

A calorimetric study

by GERMANO IANNACCHIONE, ALFREDO STRIGAZZI† and DANIELE FINOTELLO*

Department of Physics and Liquid Crystal Institute,
Kent State University, Kent, Ohio 44242
† Dipartimento di Fisica, Politecnico di Torino, and INFM,
Unità di Torino, c. Duca degli Abruzzi 24, I-10129 Torino, Italy

Using an AC-calorimetry technique, we report measurements of the heat capacity and the phase shift between the applied heating power and the resulting thermal oscillations on the thermotropic liquid crystal series of alkylcyanobiphenyl (*n*CB) above the tricritical point. Specifically, we studied the first order phase transition smectic A to isotropic as a function of substrate, under atmospheric pressure. Different combinations of sapphire, Kapton type 200H polyimide film and air, are used to vary systematically the interfaces encountered by a liquid crystal. The calorimeter uses a sapphire disk, 10 mm in diameter and 0·13 mm thick, above which the samples are placed. A second sapphire disk, or a disk-shaped Kapton film, are used to sandwich the liquid crystal. Air interface samples are droplets allowed to spread naturally on the chosen substrate. The chosen geometry is such that interface effects appear to be maximized. Striking features found in the heat capacity and the phase shift studies with 10CB and 12CB will be presented for the different interfaces.

1. Introduction

The influence of surfaces on the behaviour of liquid crystal materials is studied via the heat capacity using an AC calorimetric technique. Surface studies have been mostly performed on nematic liquid crystals [1] from a fundamental point of view, and also because these materials are used in liquid crystal display cells where surfaces play an important role in their operation. We decided to extend and investigate the role of surface interactions on the thermal properties at the smectic A to isotropic phase transition. A richness of features, involving the heat capacity peak and the phase shift between the applied heating power and the resulting thermal oscillations, are found. By choosing an appropriate geometry (either quasi-homeotropic or unidirectional planar, or hybrid), effects introduced by elastic deformations at the interface are simplified. Varying the interface in a systematic way emphasizes the interactions between a smectic liquid crystal and a particular substrate.

A brief overview of the AC calorimetric technique, as well as the sample materials and experimental construction will be presented in § 2. Section 3 contains our major results for the various interfaces involving 10CB and 12CB. The last section, 4, will summarize the results.

---

* Author for correspondence.

2. Experimental

Since its conception [2], the AC calorimetric technique has been successfully used to study phase transitions for a variety of liquid crystal systems [3–6]. It consists of the application of sinusoidally oscillating heat to a sample and measuring its thermal response. The amplitude of the induced thermal oscillations is inversely proportional to the sample heat capacity. The phase shift between the applied heat and the thermal response is related to the heat capacity and the thermal diffusive properties of the sample, hence, providing additional information about the character of the transition.

The frequency of the applied oscillations is important in simplifying the expression to calculate the heat capacity. At the operating frequency, 0·11 Hz for most of these studies, determined after extensive frequency studies at several temperatures, the heat capacity is given by [2]

$$C=\frac{P_{\mathrm{p}}}{2\omega T_{\mathrm{ac}}(\mathrm{p})}, \qquad (1)$$

where P_{p} is the applied peak power, ω is the angular frequency of the induced thermal response and $T_{\mathrm{ac}}(\mathrm{p})$ is the peak temperature oscillation induced by the applied power. The temperature oscillations, detected with a DC biased thermistor using $50\,\mu$A currents, are measured with a lock-in-amplifier in the 2f mode, so the phase shift is simultaneously acquired. With lock-in amplification and computer averaging for 15 min at every temperature, a resolution of 0·2 per cent or better in heat capacity is achieved.

A $50\,\Omega$ evanohm heater and a $10\,\mathrm{k}\Omega$ thermistor are glued to the bottom of a sapphire disk, 10 mm in diameter and 0·13 mm thick, atop which the liquid crystal samples are placed. The cell is thermally anchored, using heater and thermistor leads, and enclosed in a brass ring. The brass ring is enclosed and thermally anchored to an evacuated copper chamber resting on a water bath. The previously measured addendum heat capacity consisting of sapphire, heater and thermometer, is subtracted from measurements with liquid crystal present. Further details about the calorimeter construction and operation are given elsewhere [7].

In these measurements, two thermotropic liquid crystal members of the alkylcyanobiphenyl series, specifically 10CB and 12CB, were used. These materials undergo a first order smectic A to isotropic phase transition at 322·65 K and 330·26 K respectively, and are above the tricritical point ($n=9{\cdot}5$) [8]. The purity of the liquid crystal used was determined by chromatography to be at least 99·9 per cent. All surfaces were cleaned with acetone and completely dried before introduction of the liquid crystal. Three materials, a sapphire disk, a Kapton 200H polyimide film (0·058 mm thick), and air, were used to vary the interfaces encountered by these liquid crystals. For air interface samples, with either sapphire or Kapton (glued to the original sapphire with GE varnish) as the lower interface, a liquid crystal droplet is allowed to spread naturally over it. To remove the air interface, a second sapphire of Kapton disk was rested on the droplet, in a sandwich-like arrangement. Total sample mass was always less than 10 mg, while the dimensions are estimated to be less than $160\,\mu$m thick and 9 mm in diameter.

Alignment of the liquid crystal molecules at these interfaces can be inferred from the surface topology. At the air interface, because of the polar nature of these molecules, alignment should be homeotropic. The polyimide film has a stretch axis parallel to the surface of the film. This should favour an alignment parallel to the surface of the Kapton film [9]. For sapphire, the *c*-axis of its crystal structure is perpendicular to the surface of the disk; however, during manufacturing and despite polishing, grooves parallel to the surface may exist. Therefore, we speculate that the alignment of the smectic liquid crystal layers at the sapphire surface is almost homeotropic (slightly tilted): it is certainly homeotropic far from the clearing point [9, 10]. Further, it is known that cyanobiphenyls have a tendency to align homeotropically on inorganic substrates [11].

3. Results and discussion

Heat capacity and phase shift data are presented as a function of temperature. All data shown were obtained from cooling runs. They are grouped according to the lower substrate. For sapphire, figure 1 shows the heat capacity signature at the smectic A to isotropic phase transition for 10CB over a rather wide temperature range. A large, sharp peak is found. Expanding the temperature axis, as in figure 2, several features are clearly resolved. The sapphire–10CB–air (sa) sample exhibits a broad, asymmetric peak, with little or no pre-transitional effects. In addition, superimposed on this broad main peak, a single sharper peak and one, or probably two shoulders are found on the smectic side of the transition. The asymmetry of the broad peak, as well as the appearance of the shoulders, is reversed in temperature for heating scans, i.e. appearing on the isotropic side of the transition. This may be an indication of a temperature dependent anchoring energy [12, 13].

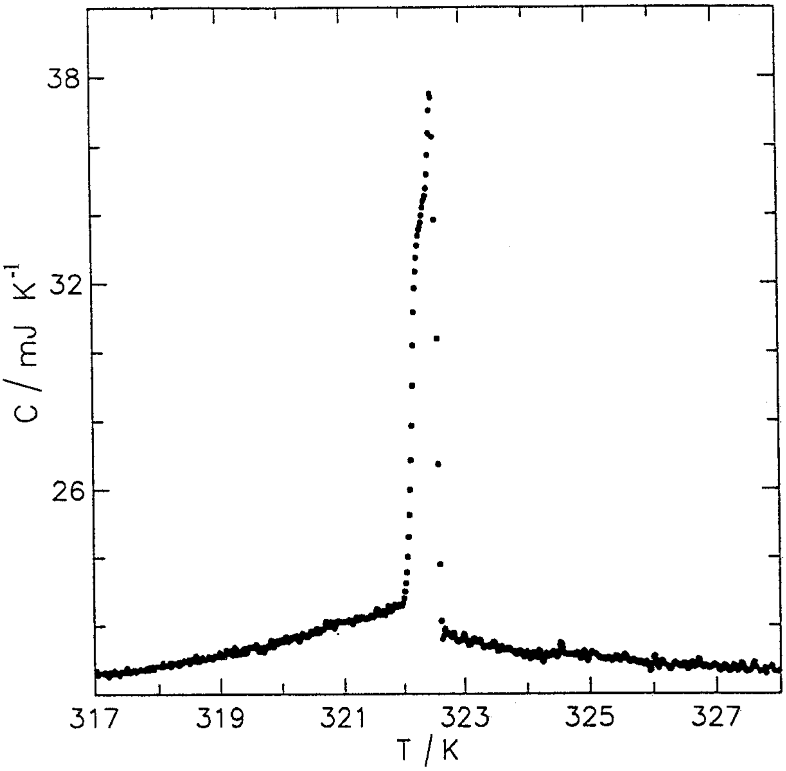

Figure 1. Total heat capacity as a function of temperature for sapphire and air interfaces in contact with 10CB.

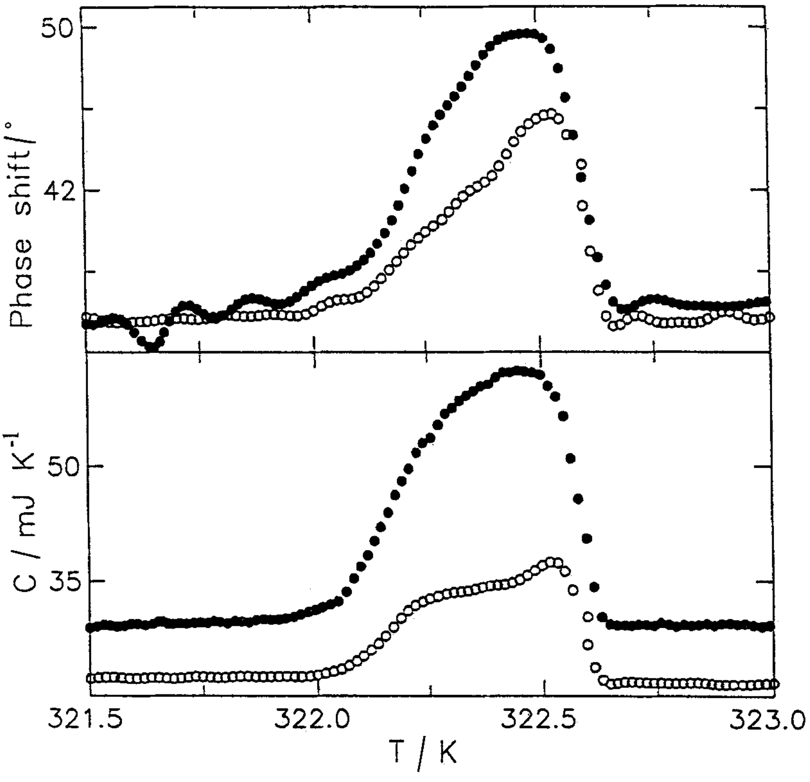

Figure 2. Total heat capacity and phase shift against temperature for the smectic A to isotropic phase transition of 10CB with sapphire as the lower substrate. The same mass of liquid crystal was used in both cases. (●) Sapphire–10CB–Kapton and (○) sapphire–10CB–air.

When a sapphire–10CB–Kapton (sK) sandwich is formed by placing a Kapton disk on top of the same liquid crystal, a main peak extending over the same temperature range as the sapphire–10CB–air sample peak, but, of greater height relative to the background, is found. The only additional feature is a single, very broad shoulder on the smectic side of the peak. It should be noted that the temperature width of the phase transition for both arrangements is the same, yet, the heat capacity peak (same liquid crystal mass) is a factor of 2 larger for the sandwich arrangement. We conjecture that this effect could be attributed to the enthalpy difference connected to the presence of distortions with disclination walls (case sK), as compared to homeotropic samples without disclinations (case sa). In fact, when the sample is sandwiched between sapphire and Kapton, the two walls give opposite boundary conditions. With a nematic sample, this would provide hybrid alignment [14], implying bend–splay deformation which in principle could exist without any disclination. But with a smectic A sample, hybrid alignment is not allowed, as the bend elastic constant goes to infinity. Thus, two opposite boundary conditions produce two opposite alignments of the smectic layers, splayed and broken by disclination walls [15].

When sapphire is replaced by Kapton as the lower interface, the heat capacity of the Kapton–10CB–air (Ka) sample shows a smooth, asymmetric and rounded peak, but no shoulders are present. This is shown in figure 3. When the same liquid crystal is sandwiched with a second Kapton disk (KK cell), the heat capacity peak is suppressed and shifts to a lower temperature compared to the Kapton–10CB–air sample. Both samples with Kapton as the lower substrate, have peak temperatures higher than those of the samples with sapphire as the lower substrate. Surprisingly, the peak height for the sandwich is smaller than that with air. This is opposite to what was found with sapphire as the lower interface. Due to the parallel alignment at the Kapton surface, we are considering the possibility of a dependence of the peak height on the position of the upper Kapton (stretch axis) as compared to the lower one. Shifts in the background heat capacity may partially reflect the torsional distortion added by the interfaces.

Phase shift measurements between the applied oscillations and the induced thermal response may indicate the region where critical fluctuations occur at a first order transition [4, 15] such as the smectic A to isotropic transition studied here. Figures 2 and 3 show the simultaneously acquired phase shift measurements for the 10CB samples. The phase shift has a peak with identical temperature width as the corresponding heat capacity peak. This suggests that the features observed are the critical fluctuations of this first order transition. In the transition region, some of the heat capacity features have an identical and in some cases more pronounced feature in the phase shift. Away from the transition region, oscillations in the phase shift have no corresponding match in the heat capacity signal. This is suggestive of changes in the thermal diffusion of the liquid crystal, which we are trying to extract from the data. Finally, the transition region seems quite broad (nearly 0·5 K) and therefore not a genuine first order transition.

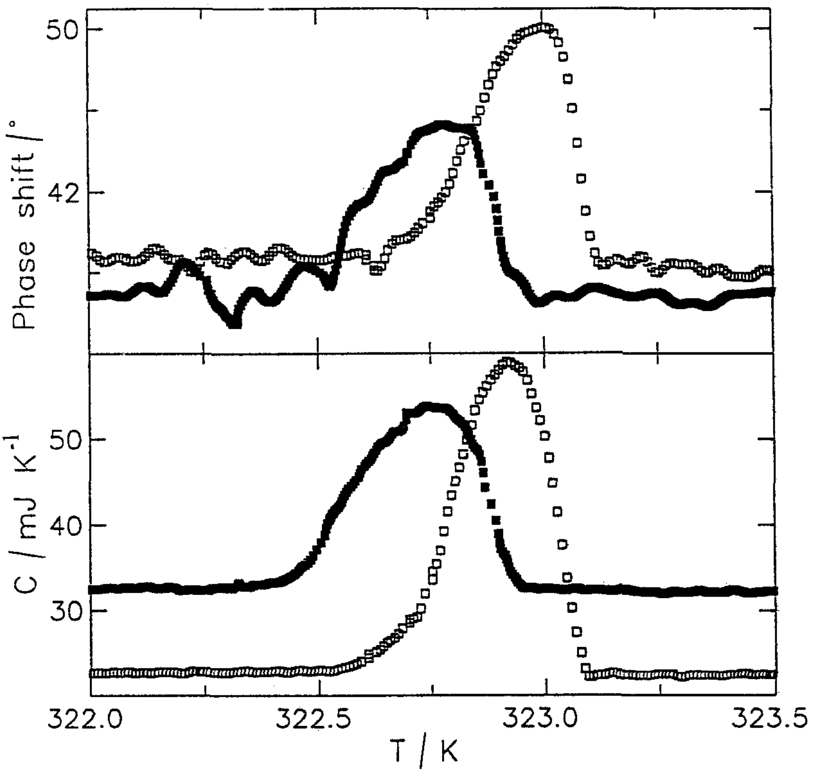

Figure 3. Total heat capacity and phase shift against temperature for the smectic A to isotropic phase transition of 10CB with Kapton as the lower substrate. The same mass of liquid crystal was used in both cases. (■) Kapton–10CB–Kapton and (□) Kapton–10CB–air.

In our studies with 12CB samples, a silane treated sapphire disk was also used to remove the air interface. Silane is well known to provide homeotropic alignment of the liquid crystal with strong anchoring at the treated surface [9, 14]. Three heat capacity runs were performed on 12CB with the following arrangements: sapphire–12CB–air (sa), sapphire–12CB–sapphire (ss) and sapphire–12CB–silane treated sapphire (sS).

The heat capacity for the sapphire–12CB–air sample, over a wide temperature range, shows a large peak, as shown in figure 4. Expanding of the temperature axis for this cooling run, shown in figure 5, allows the resolution of several unexpected features near the peak maximum. The sa sample heat capacity data exhibit features very similar to those found for 10CB, with a sharp peak and shoulders on top of a broad heat capacity peak. When a second, untreated, sapphire disk was used to remove the air interface, for the ss sample, the peaks and shoulders disappear, with no shift in temperature of the main broad peak. However, when the sS sample was studied, some of the features returned and the main peak shifted to higher temperatures. As in the 10CB case, the appearance of these additional features is reversed in temperature for heating scans. Finally, for the sS sample, an excess of specific heat, more typical of a weakly first order phase transition (as in the nematic to isotropic transition) is found. It is very likely that some of these features, in particular, the peak temperature shifts, are a direct consequence of the different smectic layer orientation found at the different boundaries. Unfortunately, no phase shift measurements are available for these samples.

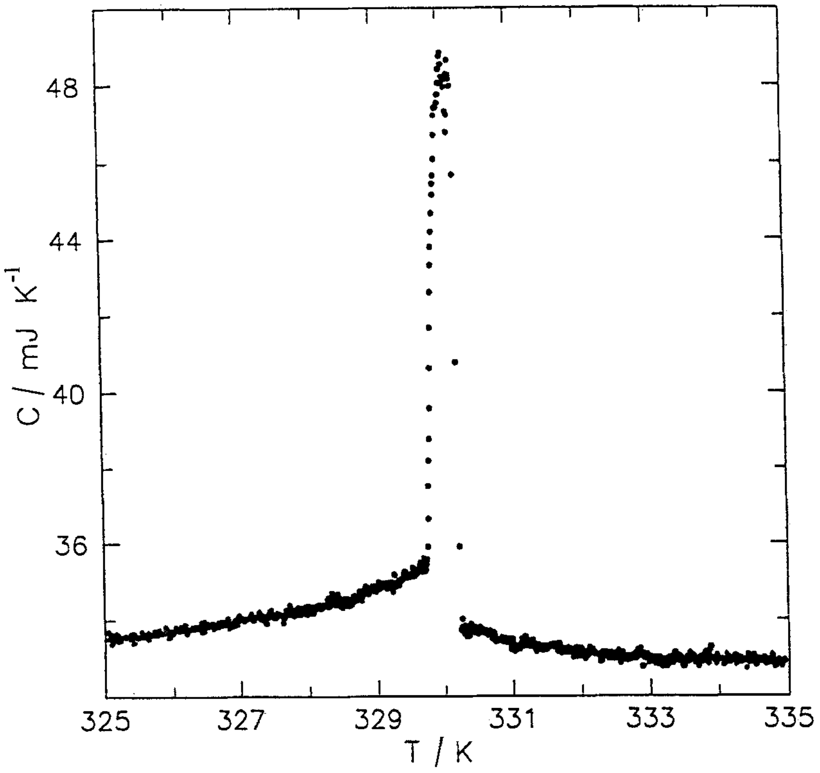

Figure 4. Total heat capacity as a function of temperature for sapphire and air interfaces in contact with 12CB.

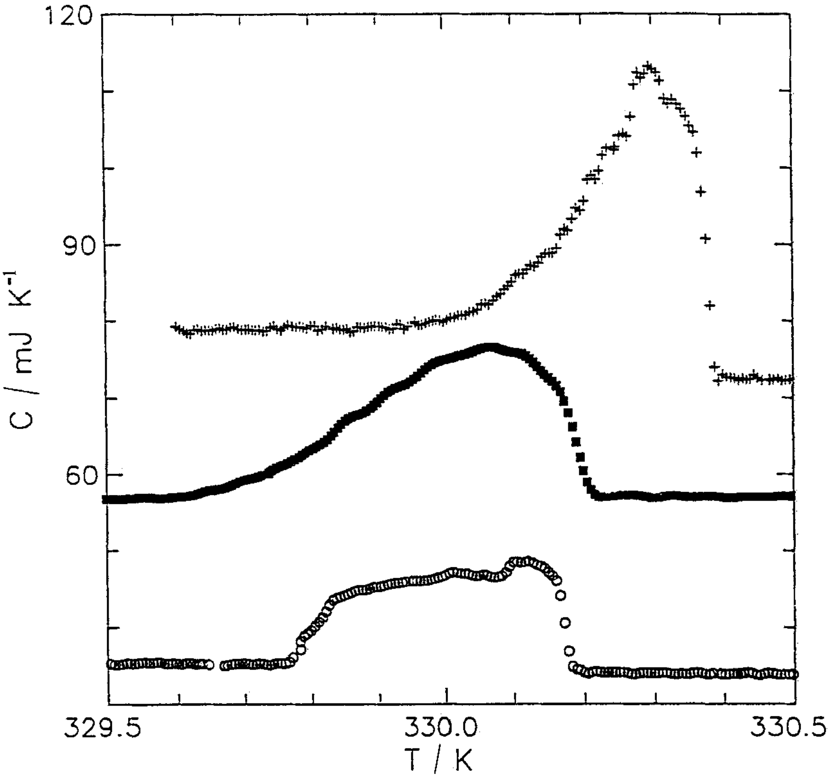

Figure 5. Total heat capacity against temperature for the smectic A to isotropic phase transition of 12CB samples with different interface configurations; (+) Sapphire/treated sapphire, (■) sapphire/sapphire and (O) sapphire/air.

Impurities are known to broaden and shift phase transitions. As previously mentioned, the purity of the samples was determined to be 99·9 per cent, and the same batch of 10CB (12CB) liquid crystal material was used for all measurements. All samples were handled identically, and, after the air interface studies were completed, the second sapphire or the Kapton disk was rested above the liquid crystal material. Thus, the impurity content would be identical for a given set of air interface measurements, and hence, not responsible for the transition temperature shifts. If an increased amount of impurities were introduced by the upper surface (in the sandwich like arrangement), the transition temperature would have to be lower. Except for the Kapton–10CB–Kapton sample, the transition temperature was either unchanged or actually increased with the presence of the upper surface (cf. sapphire–12CB–silane treated sapphire sample in figure 5). In fact, the peak temperatures of the 10CB samples are $T_{sK} = 322{\cdot}45$ K, $T_{sa} = 322{\cdot}55$ K, $T_{KK} = 322{\cdot}80$ K, and $T_{Ka} = 323{\cdot}00$ K. Therefore, we attribute the transition shifts to the order/disorder introduced by the surfaces. This is known to occur for nematic liquid crystals [16]. In the sK and Ka cases the boundary conditions are opposite (one homeotropic and one planar); in the sa case the easy directions at both walls are homeotropic, and in the KK case planar. We stress the fact that in cells with identical boundary conditions, strong anchoring lowers the distortions, whereas in cells with opposite boundary conditions, strong anchoring raises the distortions. Moreover, in the presence of elastic distortion, the sample is expected to exhibit a shift towards lower temperatures [16]. The experiment is thus consistent with the assumption that the anchoring is stronger at the sapphire substrate than at the free surface, and that the anchoring at the Kapton substrate is stronger than the average between the sapphire and the free surface itself. For the 12CB samples, the transition temperatures are $T_{ss} = 330{\cdot}05\,\mathrm{K}$, $T_{sa} = 330{\cdot}10\,\mathrm{K}$, and $T_{SS} = 330{\cdot}30\,\mathrm{K}$. This can be understood by assuming that the anchoring is strongest for the treated sapphire and weakest for the untreated sapphire.

Contrary to our original expectations, the air interface does not appear to play a major role in the formation of the peaks and shoulders of the sapphire–10CB–air sample. These features disappeared when the sapphire was replaced with Kapton as the lower interface, maintaining air as the upper interface. X-ray measurements on these liquid crystals have shown that smectic layering occurs at both the substrate and air interface for 12CB [17, 18]. This discrete layering phenomenon was, however, not observed for 10CB [17, 19]. Also, theoretical work, using a lattice–gas model, suggests that the discrete layering transition is continuous only for the first layer, the rest being first order [20]. Both X-ray measurements, as well as theoretical work, indicate that only a few layers form before the transition extends throughout the sample. The formation of the first two layers [17] occurs at temperatures well above the temperature of the main broad peak observed here. This involves, approximately, a factor of 10^{-5} of the total sample mass. Its contribution to the heat capacity could not be resolved here.

We emphasize that the features we observed are unique to the smectic A to isotropic phase transition. Measurements with bulk 5CB, 7CB and 8CB at the nematic to isotropic and smectic A to nematic phase transitions, using the same calorimeter and underlying sapphire disk, did not reveal any extra features, but merely reproduced data available in the literature [6].

4. Conclusions

We have presented heat capacity and phase shift measurements using an ac calorimetric technique on several samples of bulk 10CB and 12CB in contact with various surfaces. This study unveils a richness of effects on the heat capacity signature at the smectic A to isotropic phase transition. They are found to be strongly dependent on the surface in contact with the liquid crystal material. The natures of these features are not completely understood, but they are probably related to the orientation of the smectic layers at the different boundaries, a temperature dependence in the anchoring energies, and, the curvature of the droplet in the case of the air interface sample [21]. Wetting of the surfaces by the two phases, smectic A or isotropic, is undoubtedly different for the interfaces used (sapphire, Kapton, air). This may further contribute to some of these effects. It might be necessary to extend theoretical work done on similar nematic cell systems [16, 22] to include smectic ordering. Continued work is under way using different materials for the interfaces, better control of the sample thickness, and studies of thickness dependence.

We acknowledge useful discussions with Gregory Crawford, Satyendra Kumar, Giovanni Barbero and Amelia Sparavigna. One of us (A.S.) acknowledges the valuable assistance of I. Barishev and M. Tomilin. We are grateful to Sandy Keast for performing the purity measurements. This research was supported in part by NSF Science and Technology Center ALCOM Grant No. DMR 89-20147, and by CNR (Consiglio Nazionale delle Ricerche, Italy).

References

[1] Jerome, B., 1991, *Rep. Prog. Phys.*, **54**, 391.
[2] Sullivan, P. F., and Seidel, G., 1968, *Phys. Rev.*, **173**, 679.
[3] Geer, R., Huang, C. C., Pindak, R., and Goodby, J. W., 1989, *Phys. Rev. Lett.*, **63**, 540.
[4] Wen, X., Garland, C. W., and Wand, M. D., 1990, *Phys. Rev.* A, **42**, 6087. Garland, C. W., 1985, *Thermochim. Acta*, **88**, 127.
[5] Johnson, D. L., Hayes, C. F., deHoff, R. J., and Schantes, C. A., 1978, *Phys. Rev.* B, **18**, 4902.
[6] Iannacchione, G., and Finotello, D., 1992, *Phys. Rev. Lett.*, **69**, 2094.
[7] Steele, L. M., Iannacchione, G. S., and Finotello, D., 1993, *Revta mex. Fiz.* (submitted).
[8] Marynissen, H., Thoen, J., and van Dael, W., 1983, *Molec. Crystals liq. Crystals*, **97**, 149; 1985, *Ibid.*, **124**, 195.
[9] Bouchiat, M. A., and Langevin-Cruchon, D., 1971, *Phys. Lett.*, **34A**, 331.
[10] Chiarelli, P., Faetti, S., and Fronzoni, L., 1983, *J. Phys., France*, **44**, 1061.
[11] Ohgawara, M., Uchida, T., and Wada, M., 1981, *Molec. Crystals liq. Crystals*, **76**, 227.
[12] Yokoyama, H., Kobayashi, S., and Kamei, H., 1986, *J. appl. Phys.*, **61**, 4501.
[13] Flatischler, K., Komitov, K., Lagerwall, S. T., Stebler, B., and Strigazzi, A., 1991, *Molec. Crystals liq. Crystals*, **198**, 119.
[14] Cognard, J., 1982, *Molec. Crystals liq. Crystals*, **1**, 1.
[15] Garland, C. W., 1992, *Phase Transitions in Liquid Crystals* (NATO ASI Ser., Ser. B, Vol. 290), edited by S. Martellucci (Plenum Press).
[16] Barbero, G., Komitov, L., Petrov, M., and Strigazzi, A., 1991, *Int. J. Mod. Phys*, B, **5**, 2229.
[17] Ocko, B. M., 1990, *Phys. Rev. Lett.*, **64**, 2160.
[18] Ocko, B. M., Braslau, A., Pershan, P. S., Als-Nielson, J., and Deutsch, M., 1986, *Phys. Rev. Lett.*, **57**, 94.
[19] Pershan, P. S., 1989, *J. Phys., Paris, Colloq.*, **50**, C7-1.
[20] Pawlowska, Z., Sluckin, T. J., and Kventsel, G. F., 1988, *Phys. Rev.* A, **38**, 5342.
[21] Lavrentovich, O. D., 1992, *Phys. Rev.* A, **46**, R722.
[22] Yokoyama, H., 1988, *J. chem. Soc. Faraday Trans. 2*, **84**, 1023.